

Supporting Information for:

Elucidating the optical spectra of $[\text{Au}_{25}(\text{SR})_{18}]^q$ nanoclusters

Rosalba Juarez-Mosqueda¹ and Giannis Mpourmpakis^{1,a}

¹Department of Chemical Engineering, University of Pittsburgh, Pittsburgh, PA 15261,
USA.

^ae-mail: gmpourmp@pitt.edu

Table S1. Optimized Au-Au and Au-S bond distances within the $\text{Au}_{25}\text{S}_{18}$ inorganic core of the $[\text{Au}_{25}(\text{SR})_{18}]^q$ nanoclusters. The different types of bonds are highlighted Figure 1B. The individual bond lengths of the $\text{Au}_{\text{center}}\text{-Au}_{\text{core}}$, $\text{Au}_{\text{core}}\text{-Au}_{\text{core}}$, $\text{Au}_{\text{core}}\text{-S}$, and $\text{Au}_{\text{units}}\text{-S}$ bonds, as well as the difference relative to the corresponding bond distances in the $[\text{Au}_{25}(\text{SCH}_2\text{CH}_2\text{Ph})_{18}]^{1-}$ (values in parenthesis) are given in Å. In bold, we show the average bond distances along with their corresponding standard deviations.

	$[\text{Au}_{25}(\text{SCH}_2\text{CH}_2\text{Ph})_{18}]^{1+}$	$[\text{Au}_{25}(\text{SCH}_2\text{CH}_2\text{Ph})_{18}]^0$	$[\text{Au}_{25}(\text{SCH}_2\text{CH}_2\text{Ph})_{18}]^{1-}$	$[\text{Au}_{25}(\text{SCH}_3)_{18}]^{1-}$	$[\text{Au}_{25}(\text{SH})_{18}]^{1-}$
$\text{Au}_{\text{center}}\text{-Au}_{\text{core}}$	2.877 (-0.019)	2.859 (0.000)	2.858	2.872 (-0.014)	2.844 (0.015)
	2.898 (-0.053)	2.862 (-0.017)	2.845	2.862 (-0.016)	2.855 (-0.010)
	2.923 (-0.020)	2.901 (0.001)	2.902	2.849 (0.053)	2.829 (0.073)
	2.900 (-0.036)	2.868 (-0.003)	2.865	2.840 (0.025)	2.853 (0.012)
	2.887 (-0.068)	2.822 (-0.003)	2.819	2.829 (-0.011)	2.839 (-0.020)
	2.852 (-0.006)	2.867 (-0.020)	2.847	2.862 (-0.016)	2.834 (0.013)
	2.876 (-0.018)	2.858 (0.000)	2.858	2.872 (-0.014)	2.844 (0.014)
	2.899 (-0.054)	2.862 (-0.017)	2.845	2.863 (-0.017)	2.855 (-0.010)
	2.921 (-0.018)	2.901 (0.002)	2.903	2.849 (0.054)	2.829 (0.074)
	2.901 (-0.036)	2.868 (-0.003)	2.865	2.841 (0.024)	2.853 (0.012)
	2.887 (-0.068)	2.822 (-0.003)	2.819	2.829 (-0.010)	2.839 (-0.020)
	2.852 (-0.005)	2.867 (-0.020)	2.847	2.863 (-0.016)	2.834 (0.013)
	2.890±0.022	2.863±0.023	2.856±0.025	2.853±0.014	2.842±0.010
	$\text{Au}_{\text{core}}\text{-Au}_{\text{core}}$	3.022 (0.070)	3.057 (0.036)	3.092	2.999 (0.094)
3.117 (-0.077)		3.046 (-0.005)	3.041	3.039 (0.001)	2.978 (0.063)
3.081 (-0.094)		3.003 (-0.016)	2.987	3.036 (-0.049)	3.045 (-0.058)
2.789 (0.063)		2.816 (0.035)	2.851	2.863 (-0.012)	2.867 (-0.016)
2.857 (0.189)		2.997 (0.049)	3.046	3.059 (-0.013)	3.004 (0.042)
3.014 (0.029)		3.069 (-0.026)	3.043	3.010 (0.033)	3.033 (0.010)
2.796 (0.055)		2.817 (0.035)	2.851	2.863 (-0.012)	2.867 (-0.015)
3.486 (-0.367)		3.169 (-0.050)	3.119	3.060 (0.059)	3.022 (0.097)
2.839 (0.121)		2.941 (0.018)	2.959	3.037 (-0.078)	3.037 (-0.077)
3.437 (-0.352)		3.166 (-0.080)	3.086	3.081 (0.004)	3.014 (0.071)
2.857 (0.143)		2.938 (0.062)	3.000	3.011 (-0.011)	2.983 (0.017)

	3.404 (-0.408)	3.155 (-0.159)	2.996	3.058 (-0.062)	3.036 (-0.040)
	3.471 (-0.352)	3.169 (-0.049)	3.119	3.060 (0.059)	3.022 (0.097)
	2.803 (0.084)	2.883 (0.004)	2.886	2.863 (0.024)	2.881 (0.006)
	2.849 (0.110)	2.941 (0.019)	2.959	3.037 (-0.077)	3.037 (-0.077)
	2.805 (0.081)	2.883 (0.003)	2.886	2.862 (0.024)	2.880 (0.005)
	3.048 (-0.038)	2.998 (0.012)	3.010	3.050 (-0.040)	3.031 (-0.021)
	3.005 (0.009)	3.070 (-0.055)	3.014	2.973 (0.041)	3.021 (-0.007)
	3.049 (-0.039)	2.998 (0.013)	3.010	3.051 (-0.041)	3.031 (-0.021)
	2.831 (0.097)	2.869 (0.058)	2.928	2.868 (0.060)	2.862 (0.066)
	2.858 (0.188)	2.997 (0.049)	3.046	3.059 (-0.013)	3.004 (0.042)
	3.435 (-0.349)	3.166 (-0.080)	3.086	3.081 (0.005)	3.014 (0.072)
	3.006 (0.009)	3.070 (-0.055)	3.015	2.974 (0.041)	3.022 (-0.006)
	2.830 (0.098)	2.869 (0.059)	2.928	2.868 (0.060)	2.862 (0.066)
	3.019 (0.073)	3.056 (0.036)	3.092	2.999 (0.093)	3.027 (0.065)
	3.120 (-0.079)	3.046 (-0.005)	3.041	3.040 (0.001)	2.978 (0.063)
	3.083 (-0.097)	3.003 (-0.016)	2.987	3.036 (-0.049)	3.045 (-0.058)
	3.024 (0.019)	3.069 (-0.026)	3.043	3.011 (0.032)	3.033 (0.010)
	2.857 (0.143)	2.938 (0.062)	3.000	3.012 (-0.012)	2.983 (0.017)
	3.405 (-0.409)	3.155 (-0.159)	2.996	3.058 (-0.062)	3.036 (-0.039)
	3.040±0.225	3.012±0.105	3.004±0.072	3.001±0.073	2.989±0.063
Au _{core} -S	2.438 (0.001)	2.432 (0.006)	2.438	2.430 (0.008)	2.438 (0.000)
	2.400 (0.052)	2.429 (0.023)	2.452	2.438 (0.014)	2.444 (0.008)
	2.386 (0.048)	2.417 (0.016)	2.433	2.431 (0.002)	2.437 (-0.003)
	2.442 (-0.005)	2.437 (0.000)	2.437	2.423 (0.014)	2.447 (-0.010)
	2.427 (0.017)	2.443 (0.001)	2.444	2.424 (0.020)	2.447 (-0.003)
	2.405 (0.035)	2.421 (0.019)	2.440	2.433 (0.007)	2.444 (-0.004)
	2.439 (-0.001)	2.432 (0.006)	2.438	2.429 (0.009)	2.438 (0.000)
	2.400 (0.052)	2.429 (0.022)	2.452	2.438 (0.014)	2.444 (0.008)
	2.386 (0.047)	2.417 (0.016)	2.434	2.431 (0.003)	2.437 (-0.003)
	2.443 (-0.005)	2.436 (0.001)	2.437	2.425 (0.013)	2.447 (-0.010)
	2.428 (0.016)	2.443 (0.001)	2.444	2.424 (0.020)	2.447 (-0.003)
	2.405 (0.035)	2.421 (0.019)	2.440	2.433 (0.007)	2.444 (-0.004)
	2.416±0.021	2.430±0.009	2.441±0.006	2.430±0.005	2.443±0.004
Au _{units} -S	2.343 (-0.004)	2.339 (0.000)	2.339	2.340 (-0.001)	2.345 (-0.006)
	2.335 (0.011)	2.333 (0.012)	2.345	2.339 (0.006)	2.338 (0.008)
	2.333 (0.009)	2.349 (-0.006)	2.342	2.345 (-0.003)	2.350 (-0.008)
	2.345 (-0.001)	2.351 (-0.007)	2.344	2.343 (0.001)	2.345 (-0.001)
	2.339 (0.004)	2.340 (0.003)	2.343	2.339 (0.005)	2.341 (0.003)
	2.327 (0.025)	2.336 (0.016)	2.352	2.337 (0.016)	2.344 (0.009)
	2.334 (0.015)	2.348 (0.000)	2.349	2.343 (0.006)	2.347 (0.001)
	2.341 (0.001)	2.339 (0.002)	2.342	2.344 (-0.002)	2.341 (0.001)
	2.329 (0.006)	2.336 (-0.001)	2.335	2.344 (-0.009)	2.346 (-0.011)
	2.347 (0.001)	2.351 (-0.002)	2.348	2.342 (0.006)	2.345 (0.003)

2.339 (0.004)	2.340 (0.002)	2.343	2.336 (0.007)	2.349 (-0.006)
2.326 (0.026)	2.336 (0.016)	2.352	2.338 (0.014)	2.353 (0.000)
2.334 (0.015)	2.348 (0.000)	2.349	2.343 (0.006)	2.347 (0.001)
2.341 (0.001)	2.339 (0.002)	2.342	2.344 (-0.002)	2.341 (0.001)
2.329 (0.006)	2.336 (-0.001)	2.335	2.344 (-0.009)	2.345 (-0.010)
2.347 (0.001)	2.351 (-0.003)	2.348	2.342 (0.006)	2.345 (0.003)
2.340 (0.010)	2.345 (0.004)	2.349	2.336 (0.013)	2.349 (0.001)
2.355 (-0.004)	2.343 (0.008)	2.351	2.338 (0.013)	2.352 (-0.001)
2.343 (-0.004)	2.339 (0.000)	2.339	2.340 (-0.001)	2.345 (-0.006)
2.335 (0.010)	2.333 (0.012)	2.345	2.339 (0.006)	2.338 (0.008)
2.335 (0.007)	2.349 (-0.006)	2.342	2.345 (-0.003)	2.350 (-0.008)
2.345 (-0.002)	2.351 (-0.007)	2.344	2.343 (0.001)	2.345 (-0.001)
2.340 (0.009)	2.345 (0.004)	2.349	2.338 (0.011)	2.341 (0.008)
2.354 (-0.004)	2.343 (0.008)	2.351	2.337 (0.014)	2.344 (0.007)
2.339 ±0.008	2.343±0.006	2.345±0.005	2.341±0.003	2.345±0.004

Table S2. Atomic charges per atom type for the $[\text{Au}_{25}(\text{SR})_{18}]^q$ nanoclusters. The charges are calculated (and averaged) for the central Au atom ($\text{Au}_{\text{center}}$), the 12 Au atoms forming the Au_{12} core (Au_{core}), the 12 Au and 18 S atoms of the units (Au_{units} and S), and the corresponding number of C and H atoms in each structure. The values in parentheses correspond to the sum of the charges from all the atoms of the same kind.

	$[\text{Au}_{25}(\text{SCH}_2\text{CH}_2\text{Ph})_{18}]^{1+}$	$[\text{Au}_{25}(\text{SCH}_2\text{CH}_2\text{Ph})_{18}]^0$	$[\text{Au}_{25}(\text{SCH}_2\text{CH}_2\text{Ph})_{18}]^{1-}$	$[\text{Au}_{25}(\text{SCH}_3)_{18}]^{1-}$	$[\text{Au}_{25}(\text{SH})_{18}]^{1-}$
$\text{Au}_{\text{center}}$	-0.050	-0.075	-0.082	-0.081	-0.078
Au_{core}	0.060 (0.720)	0.050 (0.600)	0.036 (0.432)	0.032 (0.384)	0.038 (0.456)
Au_{units}	0.110 (1.320)	0.096 (1.152)	0.086 (1.032)	0.084 (1.008)	0.095 (1.140)
S	-0.131 (-2.358)	-0.154 (-2.772)	-0.167 (-3.006)	-0.148 (-2.664)	-0.162 (-2.916)
C	-0.060 (-8.640)	-0.059 (-8.496)	-0.060 (-8.640)	-0.202 (-3.636)	---
H	0.062(10.044)	0.059 (9.558)	0.057 (9.234)	0.074 (3.996)	0.022 (0.396)

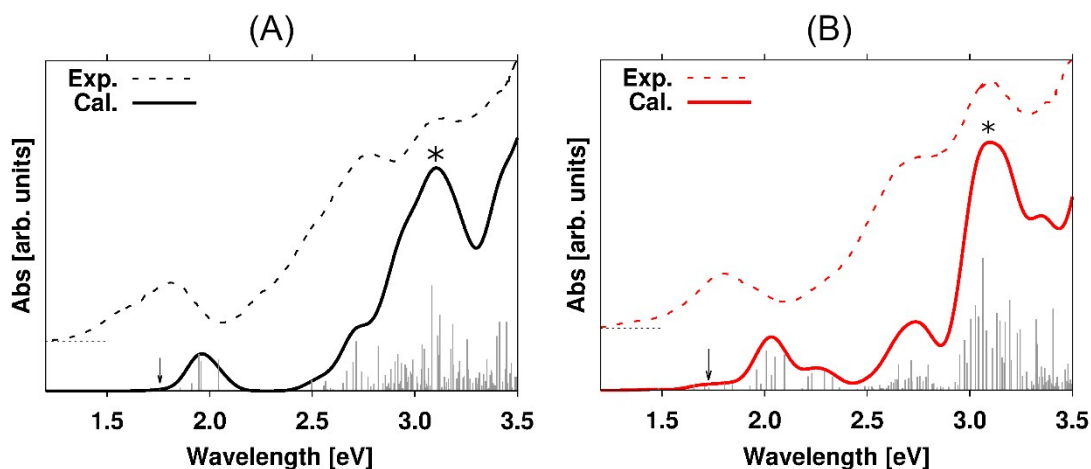


Figure S1. Calculated (solid) and experimental (dashed) absorption spectrum of the (A) $[\text{Au}_{25}(\text{SCH}_2\text{CH}_2\text{Ph})_{18}]^{1-}$ and (B) $[\text{Au}_{25}(\text{SCH}_2\text{CH}_2\text{Ph})_{18}]^0$ nanoclusters. The energies related to the HOMO-LUMO transitions are indicated with an arrow. Vertical gray lines correspond to the single oscillator strengths relative to individual electronic transitions. The calculated spectra have been broadened by a Gaussian function of 0.05 eV width and blue-shifted by 0.5 eV so the absorption peak labeled with an asterisk matches the dominant peak observed in the experimental spectrum (at ≈ 3.1 eV). Experimental spectra reproduced from reference 14.

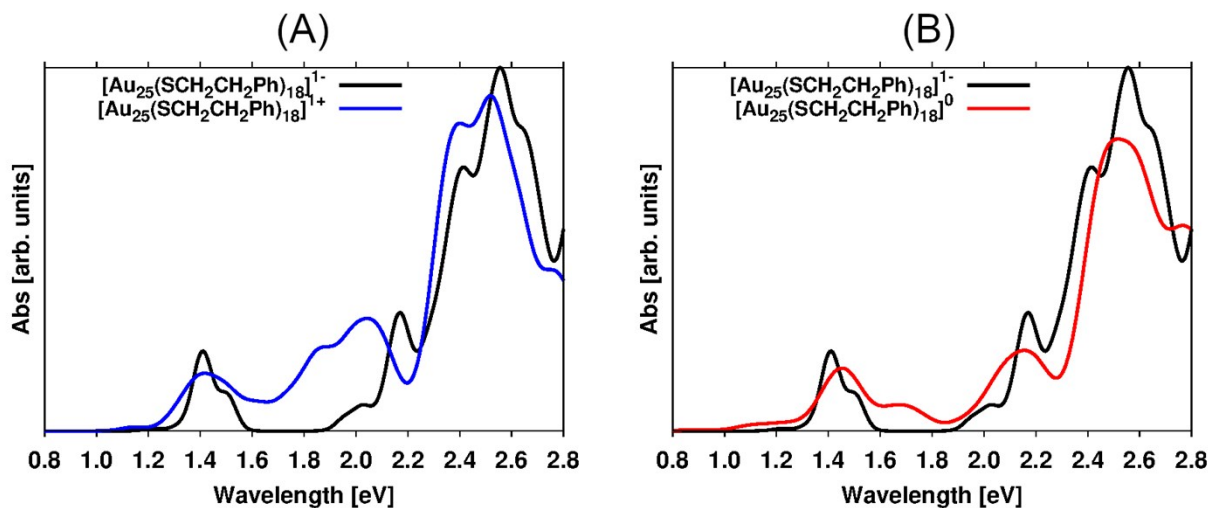


Figure S2. Comparison between the calculated absorption spectrum of the $[\text{Au}_{25}(\text{SCH}_2\text{CH}_2\text{Ph})_{18}]^{1-}$ and the spectra of (A) $[\text{Au}_{25}(\text{SCH}_2\text{CH}_2\text{Ph})_{18}]^{1+}$ and (B) $[\text{Au}_{25}(\text{SCH}_2\text{CH}_2\text{Ph})_{18}]^0$.

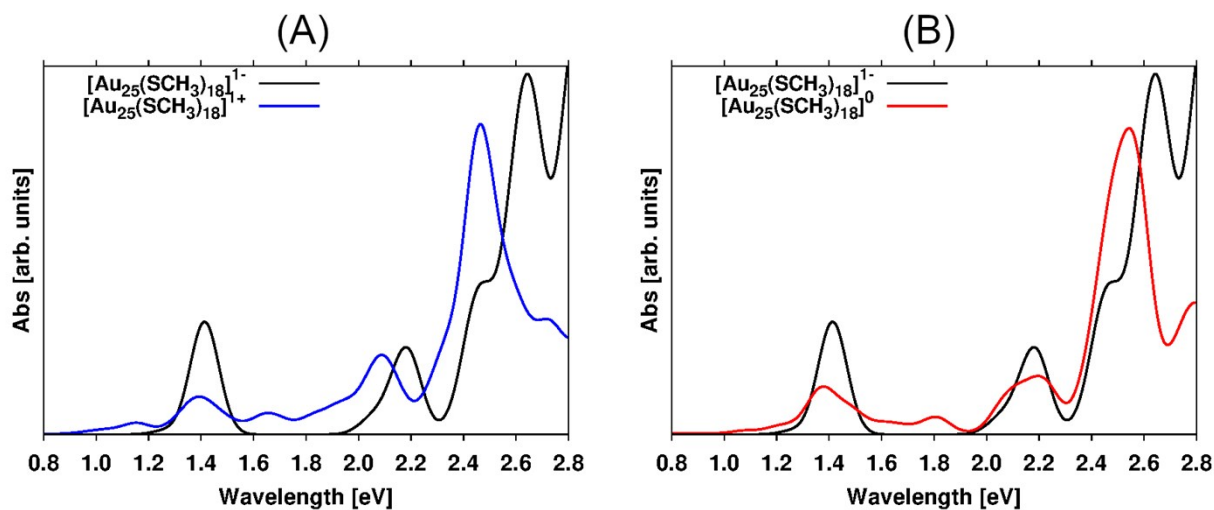


Figure S3. Comparison between the calculated absorption spectrum of the $[\text{Au}_{25}(\text{SCH}_3)_{18}]^{1-}$ and the spectra of (A) $[\text{Au}_{25}(\text{SCH}_3)_{18}]^{1+}$ and (B) $[\text{Au}_{25}(\text{SCH}_3)_{18}]^0$.

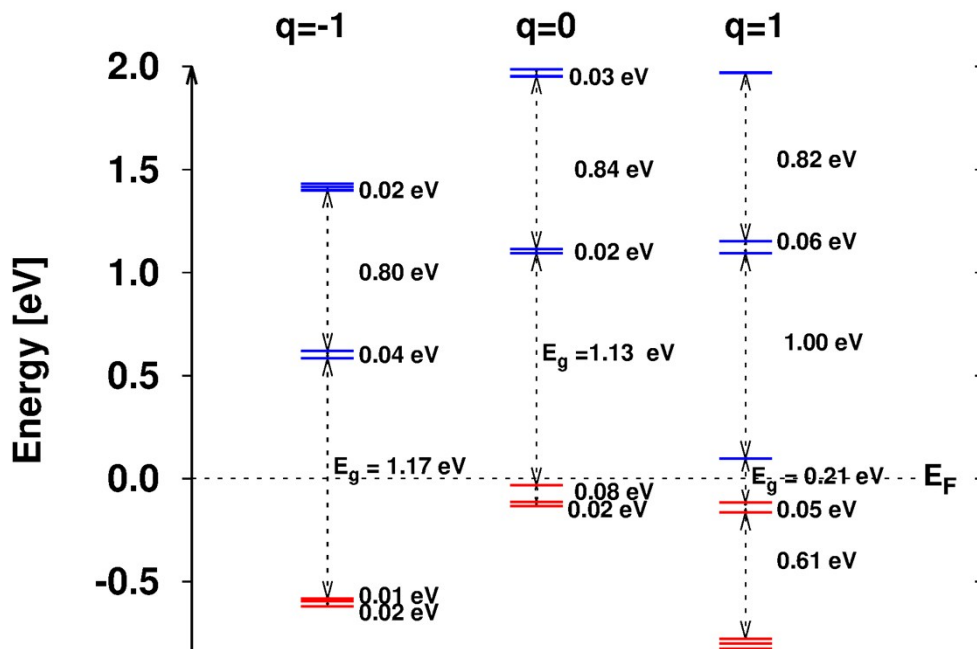


Figure S4. Energy diagram of the frontier molecular orbitals of the [Au₂₅(SCH₃)₁₈]^q nanoclusters (q=-1, 0, and 1). HOMO-2, HOMO-1, and HOMO are shown in red, and LUMO to LUMO+4 are in blue. The energy gap between HOMO-2-HOMO-1, HOMO-1-HOMO, HOMO-LUMO (E_g), LUMO-LUMO+1, LUMO+1-LUMO+2, and LUMO+2-LUMO+3 are indicated for each nanocluster. The energies of the molecular orbitals have been shifted by the corresponding nanocluster Fermi energy values: eV -1.439 (q=-1), -4.178 eV (q=0), and -6.449 eV (q=1).

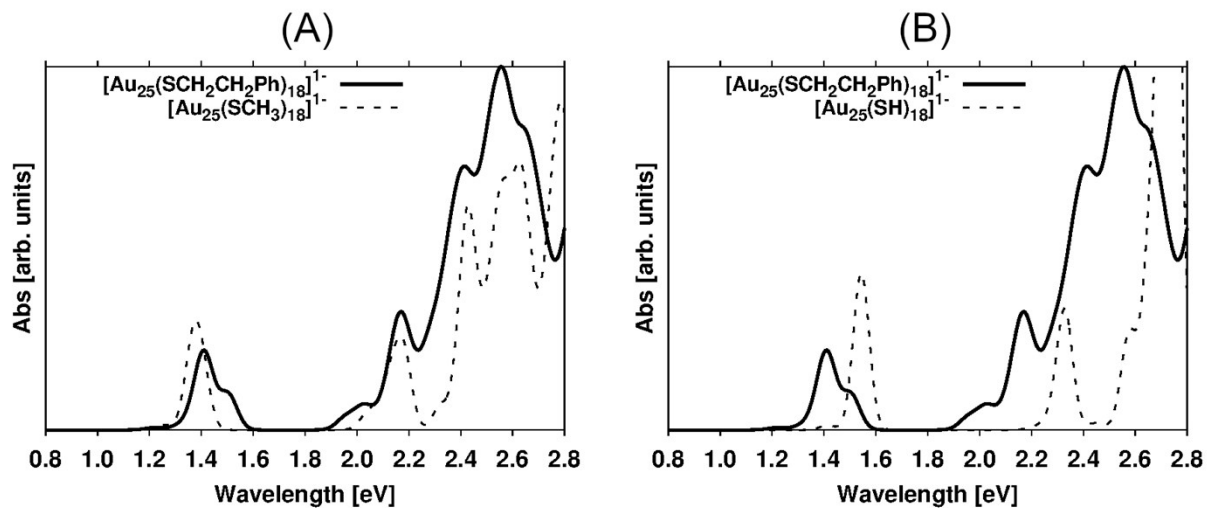


Figure S5. Comparison between the calculated absorption spectrum of the $[\text{Au}_{25}(\text{SCH}_2\text{CH}_2\text{Ph})_{18}]^{1-}$ and the spectra of (A) $[\text{Au}_{25}(\text{SCH}_3)_{18}]^{1-}$ and (B) $[\text{Au}_{25}(\text{SH})_{18}]^{1-}$.

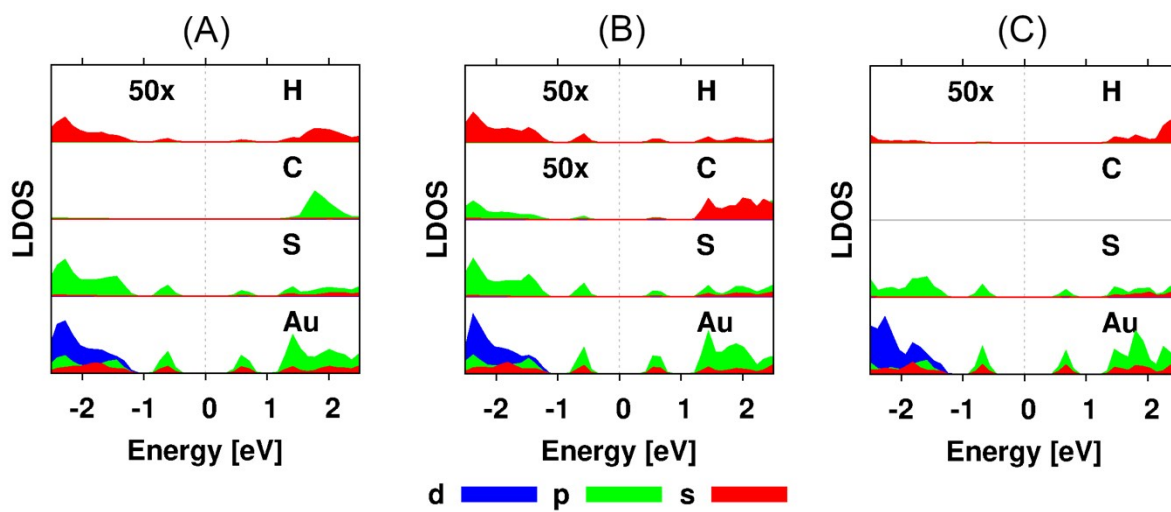


Figure S6. Local projected density of states (LPDOS) per atom type of the (A) $[\text{Au}_{25}(\text{SCH}_2\text{CH}_2\text{Ph})_{18}]^{1-}$ (B) $[\text{Au}_{25}(\text{SCH}_3)_{18}]^{1-}$, and (C) $[\text{Au}_{25}(\text{SH})_{18}]^{1-}$ nanoclusters.

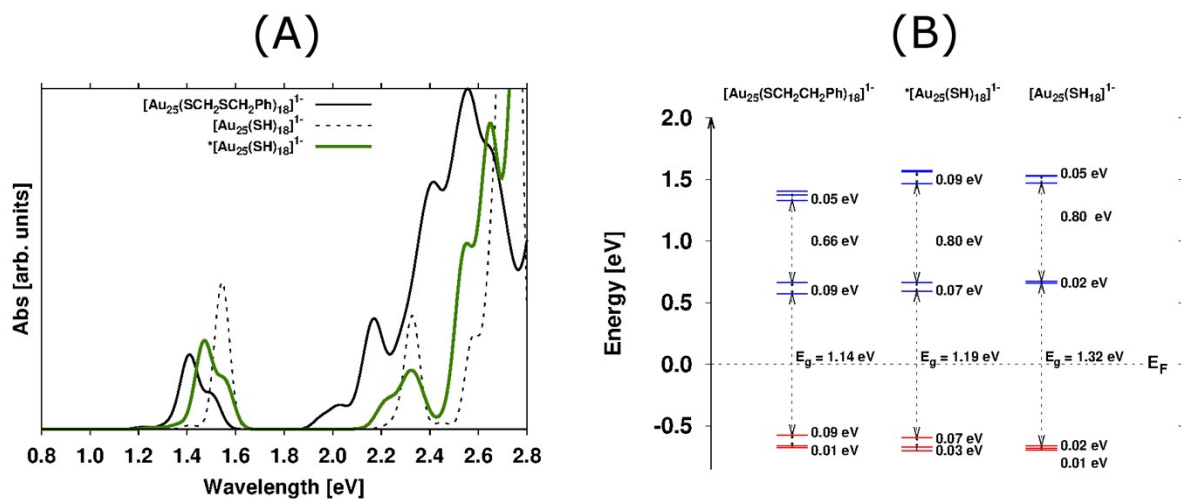


Figure S7. (A) Comparison between the calculated absorption spectrum of the optimized $[\text{Au}_{25}(\text{SCH}_2\text{CH}_2\text{Ph})_{18}]^{1-}$ (solid black) and $[\text{Au}_{25}(\text{SH})_{18}]^{1-}$ nanoclusters (dashed black). The green plot corresponds to the spectrum of the $^*[\text{Au}_{25}(\text{SH})_{18}]^{1-}$ nanocluster with the geometry of the $\text{Au}_{25}\text{S}_{18}$ core of $[\text{Au}_{25}(\text{SCH}_2\text{CH}_2\text{Ph})_{18}]^{1-}$. In $^*[\text{Au}_{25}(\text{SH})_{18}]^{1-}$ only the position of the H atoms were allowed to relax during optimization. (B) Energy of the frontier molecular orbitals of optimized $[\text{Au}_{25}(\text{SCH}_2\text{CH}_2\text{Ph})_{18}]^{1-}$ (left) and $[\text{Au}_{25}(\text{SH})_{18}]^{1-}$ (right) nanoclusters. The energy diagram of $^*[\text{Au}_{25}(\text{SH})_{18}]^{1-}$ (middle) corresponds to the aforementioned constrained system. HOMO-2, HOMO-1, and HOMO are shown in red, and LUMO to LUMO+4 are in blue. The energy gap between HOMO-2-HOMO-1, HOMO-1-HOMO, HOMO-LUMO (E_g), LUMO-LUMO+1, LUMO+1-LUMO+2, and LUMO+2-LUMO+3 are indicated for each nanocluster.

Table S3. Energy, oscillator strength, and orbital contributions of the main electronic transitions occurring below 2.5 eV in the spectrum of $[\text{Au}_{25}(\text{SCH}_2\text{CH}_2\text{Ph})_{18}]^{1-}$ nanocluster. The relative contribution of molecular orbitals to a given oscillator strength is indicated in percentage. The letters α , β , γ' , and γ are used to distinguish between the main absorption peaks in the spectra shown in Figure 5.

$[\text{Au}_{25}(\text{SCH}_2\text{CH}_2\text{Ph})_{18}]^{1-}$			
Peak	Energy	Osc. Str.	Transitions
α	1.217	8.23E-04	HOMO \rightarrow LUMO (91 %)
β	1.315	1.42E-03	HOMO-2 \rightarrow LUMO (79 %) HOMO \rightarrow LUMO+1 (13 %)
	1.372	3.12E-03	HOMO-1 \rightarrow LUMO+1 (65%) HOMO \rightarrow LUMO+1 (24%)
	1.406	1.50E-02	HOMO-1 \rightarrow LUMO (52 %) HOMO \rightarrow LUMO+1 (26 %)
	1.418	1.19E-02	HOMO-1 \rightarrow LUMO+1 (11 %)
			HOMO-1 \rightarrow LUMO (39 %)
HOMO \rightarrow LUMO+1 (25 %) HOMO-1 \rightarrow LUMO+1 (22%)			
β'	1.503	1.27E-02	HOMO-2 \rightarrow LUMO+1 (85%)
γ'	1.956	4.30E-03	HOMO \rightarrow LUMO+2 (73 %) HOMO \rightarrow LUMO+4 (13 %)
	2.016	2.03E-03	HOMO \rightarrow LUMO+3 (34 %)
			HOMO \rightarrow LUMO+4 (30 %)
			HOMO-5 \rightarrow LUMO (12 %)
	2.025	4.10E-03	HOMO \rightarrow LUMO+4 (28 %)
			HOMO-5 \rightarrow LUMO (22 %)
			HOMO \rightarrow LUMO+3 (15 %)
			HOMO-6 \rightarrow LUMO (11 %)
	2.034	8.52E-04	HOMO-1 \rightarrow LUMO+3 (36 %)
			HOMO-2 \rightarrow LUMO+2 (26 %)
HOMO-1 \rightarrow LUMO+2 (22 %)			
2.048	1.23E-03	HOMO-2 \rightarrow LUMO+2 (29 %)	
		HOMO-1 \rightarrow LUMO+2 (26 %)	
		HOMO \rightarrow LUMO+4 (13 %)	
2.059	7.80E-04	HOMO-2 \rightarrow LUMO+3 (10 %)	
		HOMO-6 \rightarrow LUMO (57 %)	
		HOMO-5 \rightarrow LUMO (16 %) HOMO-1 \rightarrow LUMO+3 (13 %)	
γ	2.109	3.16E-03	HOMO-1 \rightarrow LUMO+4 (36 %)
			HOMO-2 \rightarrow LUMO+3 (23 %)
			HOMO-6 \rightarrow LUMO+1 (16 %)
	2.127	8.10E-03	HOMO-2 \rightarrow LUMO+4 (10 %)
			HOMO-5 \rightarrow LUMO+1 (54 %) HOMO-2 \rightarrow LUMO+4 (13 %)
2.158	1.17E-02	HOMO-2 \rightarrow LUMO+3 (11 %)	
		HOMO-7 \rightarrow LUMO (28 %) HOMO-5 \rightarrow LUMO+1 (24 %)	
2.173	2.00E-02	HOMO-6 \rightarrow LUMO+1 (20 %) HOMO-7 \rightarrow LUMO (40 %) HOMO-6 \rightarrow LUMO+1 (27 %)	

Table S4. Energy, oscillator strength, and orbital contributions of the main electronic transitions occurring below 2.5 eV in the spectrum of $[\text{Au}_{25}(\text{SCH}_2\text{CH}_2\text{Ph})_{18}]^0$ and $[\text{Au}_{25}(\text{SCH}_2\text{CH}_2\text{Ph})_{18}]^{1+}$ nanoclusters. The relative contribution of molecular orbitals to a given oscillator strength is indicated in percentage. The letters α , β , β' , β'' , γ' , and γ are used to distinguish between the main absorption peaks in the spectra shown in Figure 5.

$[\text{Au}_{25}(\text{SCH}_2\text{CH}_2\text{Ph})_{18}]^0$				$[\text{Au}_{25}(\text{SCH}_2\text{CH}_2\text{Ph})_{18}]^{1+}$			
Peak	Energy	Osc. Str.	transitions	Peak	Energy	Osc. Str.	transitions
α	1.075	1.62E-03	HOMO*-8 \rightarrow HOMO* (47 %)	α	0.511	1.00E-08	HOMO \rightarrow LUMO (96%)
	1.127	1.33E-03	HOMO*-9 \rightarrow HOMO* (37 %)		0.544	1.00E-07	HOMO-1 \rightarrow LUMO (96%)
	1.147	8.26E-04	HOMO* \rightarrow LUMO (23 %)		1.143	1.78E-03	HOMO-2 \rightarrow LUMO (94 %)
	1.155	1.94E-04	HOMO* \rightarrow LUMO (16 %)		1.188	2.42E-04	HOMO-4 \rightarrow LUMO (91 %)
	1.224	2.52E-03	HOMO* \rightarrow LUMO+1 (40 %)	β	1.296	4.35E-03	HOMO-7 \rightarrow LUMO (75 %)
	1.263	1.78E-03	HOMO*-13 \rightarrow HOMO* (47 %)		1.324	2.44E-03	HOMO \rightarrow LUMO+1 (16 %)
β	1.348	1.41E-03	HOMO*-2 \rightarrow LUMO (51 %)				HOMO-1 \rightarrow LUMO+1 (53 %)
			HOMO*-1 \rightarrow LUMO+1 (34 %)				HOMO-8 \rightarrow LUMO (29 %)
	1.381	6.72E-03	HOMO*-1 \rightarrow LUMO+1 (40 %)				HOMO \rightarrow LUMO+2 (14 %)
			HOMO*-1 \rightarrow LUMO (19 %)	1.351	2.15E-03		HOMO-8 \rightarrow LUMO (41 %)
			HOMO*-2 \rightarrow LUMO+1 (11 %)				HOMO-9 \rightarrow LUMO (28 %)
	1.400	2.18E-03	HOMO*-1 \rightarrow LUMO (37 %)				HOMO \rightarrow LUMO+2 (10%)
	1.427	1.28E-02	HOMO*-1 \rightarrow LUMO (21 %)	1.366	8.51E-03		HOMO \rightarrow LUMO+1 (41 %)
			HOMO*-2 \rightarrow LUMO (19 %)				HOMO \rightarrow LUMO+2 (14 %)
			HOMO*-1 \rightarrow LUMO+1 (13 %)				HOMO-8 \rightarrow LUMO (13 %)
	1.453	4.75E-03	HOMO*-2 \rightarrow LUMO+1 (45 %)				HOMO-9 \rightarrow LUMO (13 %)
1.470	1.13E-02	HOMO*-16 \rightarrow HOMO* (39 %)	1.366	8.51E-03		HOMO-7 \rightarrow LUMO (11 %)	
β'	1.516	1.17E-02	HOMO*-2 \rightarrow LUMO+1 (29 %)	1.408	6.47E-03		HOMO-9 \rightarrow LUMO (48 %)
β''	1.631	4.44E-03	HOMO*-22 \rightarrow HOMO* (26 %)	1.420	1.15E-02		HOMO \rightarrow LUMO+1 (20 %)
			HOMO*-19 \rightarrow HOMO* (16 %)				HOMO \rightarrow LUMO+2 (52 %)
	1.649	5.38E-03	HOMO*-23 \rightarrow HOMO* (44 %)				HOMO-1 \rightarrow LUMO+1 (18 %)
	1.711	5.82E-03	HOMO*-25 \rightarrow HOMO* (40 %)	β'	1.493	9.70E-03	HOMO-1 \rightarrow LUMO+2 (48 %)
	1.750	4.29E-03	HOMO*-26 \rightarrow HOMO* (41 %)				HOMO-11 \rightarrow LUMO (24 %)
	1.783	1.06E-03	HOMO*-29 \rightarrow HOMO* (47 %)	1.494	4.95E-03		HOMO-11 \rightarrow LUMO (51 %)
γ'	1.908	1.32E-03	HOMO*-37 \rightarrow HOMO* (43 %)				HOMO-1 \rightarrow LUMO+2 (23 %)
	1.927	1.22E-03	HOMO*-38 \rightarrow HOMO* (48 %)				HOMO-10 \rightarrow LUMO (10 %)
	1.942	1.24E-03	HOMO*-42 \rightarrow HOMO* (30 %)	β''	1.508	2.53E-03	HOMO-12 \rightarrow LUMO (92 %)
			HOMO*-41 \rightarrow HOMO* (18 %)		1.550	2.04E-03	
	1.947	4.84E-04	HOMO*-41 \rightarrow HOMO* (26 %)				HOMO-15 \rightarrow LUMO (40 %)
			HOMO*-42 \rightarrow HOMO* (19 %)	1.578	4.04E-03		HOMO-15 \rightarrow LUMO (44 %)
	1.981	1.68E-03	HOMO* \rightarrow LUMO+2 (28 %)				HOMO-13 \rightarrow LUMO (30 %)
			HOMO*-46 \rightarrow HOMO (18 %)	1.585	3.23E-06		HOMO-14 \rightarrow LUMO (90 %)
	1.986	8.25E-04	HOMO*-46 \rightarrow HOMO* (28 %)	1.612	2.37E-04		HOMO-16 \rightarrow LUMO (63 %)
			HOMO* \rightarrow LUMO+2 (12 %)				HOMO-19 \rightarrow LUMO (24 %)
1.992	5.58E-04	HOMO*-45 \rightarrow HOMO* (27 %)	1.613	3.36E-03		HOMO-17 \rightarrow LUMO (73 %)	
		HOMO*-48 \rightarrow HOMO* (13 %)	1.634	4.43E-05		HOMO-13 \rightarrow LUMO (12 %)	
1.997	6.70E-04	HOMO*-48 \rightarrow HOMO* (32 %)				HOMO-19 \rightarrow LUMO (67 %)	
		HOMO*-45 \rightarrow HOMO* (11 %)	1.638	5.94E-03		HOMO-16 \rightarrow LUMO (19 %)	
γ	2.024	1.36E-03	HOMO*-50 \rightarrow HOMO* (25 %)	1.658	6.66E-04		HOMO-18 \rightarrow LUMO (82 %)
			HOMO* \rightarrow LUMO+3 (14 %)				HOMO-20 \rightarrow LUMO (89 %)
	2.037	2.86E-03	HOMO*-50 \rightarrow HOMO* (19 %)	γ'	1.710	2.85E-03	HOMO-25 \rightarrow LUMO (50 %)
			HOMO*-5 \rightarrow LUMO (16 %)				HOMO-23 \rightarrow LUMO (40 %)
			HOMO* \rightarrow LUMO+3 (12 %)	1.727	3.65E-03		HOMO-27 \rightarrow LUMO (37%)
	2.048	2.28E-03	HOMO*-52 \rightarrow HOMO* (40 %)				HOMO-25 \rightarrow LUMO (22 %)
	2.056	3.60E-03	HOMO* \rightarrow LUMO+4 (18 %)				HOMO-29 \rightarrow LUMO (19%)
			HOMO*-6 \rightarrow LUMO (12 %)				HOMO-23 \rightarrow LUMO (17%)
	2.067	3.47E-03	HOMO*-54 \rightarrow HOMO* (44 %)	1.739	1.88E-04		HOMO-28 \rightarrow LUMO (66 %)
	2.072	8.26E-03	HOMO*-5 \rightarrow LUMO (48 %)				HOMO-26 \rightarrow LUMO (20 %)
	2.092	7.73E-04	HOMO*-6 \rightarrow LUMO (32 %)	1.741	4.32E-03		HOMO-27 \rightarrow LUMO (51 %)
			HOMO*-1 \rightarrow LUMO+3 (18 %)				HOMO-25 \rightarrow LUMO (16 %)
			HOMO*-5 \rightarrow LUMO+1 (18 %)	1.761	3.06E-03		HOMO-30 \rightarrow LUMO (40 %)
	2.105	3.34E-03	HOMO*-5 \rightarrow LUMO+1 (53 %)				HOMO-29 \rightarrow LUMO (36 %)
			HOMO*-6 \rightarrow LUMO (15 %)	1.768	1.40E-03		HOMO-23 \rightarrow LUMO (15 %)
2.123	3.86E-03	HOMO*-6 \rightarrow LUMO+1 (59 %)				HOMO-30 \rightarrow LUMO (36 %)	
		HOMO*-1 \rightarrow LUMO+2 (18 %)				HOMO-32 \rightarrow LUMO (33%)	
2.134	9.81E-03	HOMO*-59 \rightarrow HOMO* (14 %)				HOMO-29 \rightarrow LUMO (14 %)	
2.137	2.82E-03	HOMO*-59 \rightarrow HOMO* (35 %)	1.801	5.86E-03		HOMO-32 \rightarrow LUMO (54 %)	

2.165	4.45E-03	HOMO*-7→ LUMO (20 %) HOMO*-7→ LUMO+1 (59 %)	1.828	5.39E-04	HOMO-30→ LUMO (14%) HOMO-29→ LUMO (12 %)
2.176	4.84E-03	HOMO*-1→ LUMO+4 (14 %) HOMO*-1→ LUMO+2 (24 %)	1.831	1.18E-02	HOMO-35→ LUMO (68 %) HOMO-34→ LUMO (22 %)
2.206	4.27E-03	HOMO*-63→ HOMO* (15 %)	1.852	2.24E-03	HOMO-36→ LUMO (93 %)
2.207	1.33E-03	HOMO*-66→ HOMO* (33 %) HOMO*-2→LUMO+3 (15 %)	1.865	9.73E-03	HOMO-39→ LUMO (92 %) HOMO-40→ LUMO (47 %)
2.209	4.03E-03	HOMO*-2→ LUMO+4 (14 %) HOMO*-2→ LUMO+3 (28 %)	1.875	1.49E-03	HOMO-41→ LUMO (32 %) HOMO-37→ LUMO (14 %)
2.216	8.35E-03	HOMO*-67→ HOMO* (17 %) HOMO*-2→LUMO+4 (10 %)	1.876	3.87E-03	HOMO-42→ LUMO (58 %) HOMO-41→ LUMO (14 %)
		HOMO*-2→ LUMO+4 (31 %)	1.876	3.87E-03	HOMO-43→ LUMO (13 %) HOMO-41→ LUMO (33 %)
			1.886	2.85E-03	HOMO-37→ LUMO (25 %) HOMO-42→ LUMO (23 %)
			1.916	2.09E-03	HOMO-37→ LUMO (33 %) HOMO-40→ LUMO (31 %)
			1.919	2.50E-03	HOMO-45→ LUMO (22 %) HOMO-45→ LUMO (44 %)
			1.920	3.76E-05	HOMO-50→ LUMO (30 %) HOMO-48→ LUMO (84 %)
			1.920	3.76E-05	HOMO-47→ LUMO (35 %) HOMO-46→ LUMO (30%) HOMO-49→ LUMO (18 %)
γ	1.950	8.44E-03	1.950	8.44E-03	HOMO-50→ LUMO (45 %) HOMO-45→ LUMO (15%) HOMO-54→ LUMO (11 %)
			1.962	7.52E-03	HOMO-3→ LUMO+1 (65 %)
			1.970	9.03E-04	HOMO-54→ LUMO (65 %)
			1.985	9.26E-03	HOMO-5→ LUMO+1 (55 %) HOMO-58→ LUMO (14 %)
			1.999	1.39E-04	HOMO-57→ LUMO (63 %) HOMO-55→ LUMO (13%)
			2.000	2.51E-03	HOMO-56→ LUMO (41%) HOMO-52→ LUMO (15 %)
			2.007	7.95E-03	HOMO-56→ LUMO (25 %) HOMO-3→ LUMO+2 (16 %)
			2.014	2.85E-03	HOMO-52→ LUMO (13 %) HOMO-58→ LUMO (11 %)
			2.014	8.84E-04	HOMO-58→ LUMO (24%) HOMO-61→ LUMO (16 %)
			2.014	8.84E-04	HOMO-4→ LUMO+1 (11%) HOMO-52→ LUMO (10 %)
			2.030	8.99E-03	HOMO-6→ LUMO+1 (7%) HOMO-4→ LUMO+1 (42 %)
			2.036	3.68E-04	HOMO-59→ LUMO (20 %) HOMO-60→ LUMO (44 %)
			2.050	3.20E-03	HOMO-60→ LUMO (44 %) HOMO-3→ LUMO+2 (15 %)
			2.068	1.24E-03	HOMO-61→ LUMO (9 %) HOMO-61→ LUMO (43 %)
			2.078	5.23E-03	HOMO-3→ LUMO+2 (18 %) HOMO-58→ LUMO (10 %)
			2.080	3.31E-03	HOMO-5→ LUMO+2 (40 %) HOMO-61→ LUMO (17 %)
			2.081	1.93E-02	HOMO-3→ LUMO+2 (13 %) HOMO-63→ LUMO (95 %)
			2.136	1.84E-02	HOMO-60→ LUMO (23 %) HOMO-6→ LUMO+1 (17 %)
					HOMO-52→ LUMO (12 %) HOMO-5→ LUMO+2 (11 %)
					HOMO-62→ LUMO (27 %) HOMO-2→ LUMO+2 (21 %)
					HOMO-4→ LUMO+2 (19%) HOMO-5→ LUMO+2 (19 %)
					HOMO-6→ LUMO+1 (17%) HOMO-60→ LUMO (13 %)
					HOMO→ LUMO+3 (11 %) HOMO-6→ LUMO+2 (81 %)

Table S5. Energy, oscillator strength, and orbital contributions of the main electronic transitions occurring below 2.5 eV in the spectrum of $[\text{Au}_{25}(\text{SCH}_3)_{18}]^{1-}$ and $[\text{Au}_{25}(\text{SH})_{18}]^{1-}$ nanoclusters. The relative contribution of molecular orbitals to a given oscillator strength is indicated in percentage. The letters α , β , γ' , and γ are used to distinguish between the main absorption peaks in the spectra shown in Figure 11.

$[\text{Au}_{25}(\text{SCH}_3)_{18}]^{1-}$				$[\text{Au}_{25}(\text{SH})_{18}]^{1-}$			
Peak	Energy	Osc. Str.	transitions	Peak	Energy	Osc. Str.	transitions
α	1.250	4.75E-04	HOMO \rightarrow LUMO (58 %)	α	1.398	2.76E-04	HOMO \rightarrow LUMO+1 (74 %)
			HOMO-2 \rightarrow LUMO (15 %)				HOMO-2 \rightarrow LUMO (16 %)
			HOMO-1 \rightarrow LUMO+1 (16%)				HOMO-1 \rightarrow LUMO (90 %)
	1.255	6.22E-04	HOMO \rightarrow LUMO+1 (30 %)		1.405	2.67E-04	HOMO \rightarrow LUMO (40 %)
			HOMO-2 \rightarrow LUMO (26 %)				HOMO-2 \rightarrow LUMO+1 (54 %)
			HOMO-1 \rightarrow LUMO+1 (59 %)				
	1.277	4.73E-04	HOMO-2 \rightarrow LUMO (29%)	β	1.535	1.63E-02	HOMO-2 \rightarrow LUMO (43 %)
							HOMO \rightarrow LUMO+1 (18 %)
							HOMO \rightarrow LUMO (16 %)
β	1.359	1.45E-02	HOMO \rightarrow LUMO (31 %)		1.546	1.75E-02	HOMO-2 \rightarrow LUMO+1 (12 %)
			HOMO \rightarrow LUMO+1 (35 %)				HOMO \rightarrow LUMO (32 %)
			HOMO-2 \rightarrow LUMO (17 %)				HOMO-2 \rightarrow LUMO+1 (30 %)
	1.380	1.42E-02	HOMO-1 \rightarrow LUMO+1 (11 %)		1.551	1.56E-02	HOMO-2 \rightarrow LUMO (24 %)
			HOMO-1 \rightarrow LUMO (57%)				HOMO-1 \rightarrow LUMO+1 (83 %)
			HOMO \rightarrow LUMO+1 (17 %)				
	1.408	1.25E-02	HOMO-2 \rightarrow LUMO+1 (81 %)	γ	2.189	1.56E-04	HOMO-1 \rightarrow LUMO+2 (51 %)
							HOMO-1 \rightarrow LUMO+4 (16 %)
							HOMO \rightarrow LUMO+3 (36 %)
γ'	2.009	4.80E-04	HOMO \rightarrow LUMO+2 (77 %)		2.211	1.98E-04	HOMO-2 \rightarrow LUMO+2 (27 %)
			HOMO-1 \rightarrow LUMO+2 (10 %)				HOMO-1 \rightarrow LUMO+2 (11 %)
			HOMO-1 \rightarrow LUMO+3 (62 %)				HOMO \rightarrow LUMO+4 (31 %)
	2.036	8.02E-04	HOMO-5 \rightarrow LUMO (81 %)		2.245	4.24E-04	HOMO-5 \rightarrow LUMO+1 (23 %)
			HOMO-2 \rightarrow LUMO+2 (10 %)				HOMO \rightarrow LUMO+2 (12 %)
			HOMO \rightarrow LUMO+3 (38 %)				HOMO-1 \rightarrow LUMO+3 (10 %)
	2.050	6.38E-04	HOMO \rightarrow LUMO+5 (12 %)		2.250	4.40E-04	HOMO-1 \rightarrow LUMO+4 (19 %)
			HOMO-6 \rightarrow LUMO (47 %)				HOMO-6 \rightarrow LUMO (19 %)
			HOMO \rightarrow LUMO+5 (18 %)				HOMO-5 \rightarrow LUMO (14 %)
	2.059	6.10E-04	HOMO-2 \rightarrow LUMO+2 (13 %)		2.260	6.90E-04	HOMO-2 \rightarrow LUMO+4 (11 %)
			HOMO \rightarrow LUMO+3 (11 %)				HOMO-5 \rightarrow LUMO (34 %)
			HOMO-1 \rightarrow LUMO+2 (29 %)				HOMO-6 \rightarrow LUMO (29 %)
	2.070	1.11E-03	HOMO-2 \rightarrow LUMO+3 (26 %)		2.265	7.48E-04	HOMO-2 \rightarrow LUMO+3 (14 %)
			HOMO-5 \rightarrow LUMO+1 (23 %)				HOMO-5 \rightarrow LUMO (23 %)
			HOMO-5 \rightarrow LUMO+1 (34 %)				HOMO-7 \rightarrow LUMO (17 %)
	2.079	8.58E-04	HOMO-1 \rightarrow LUMO+5 (24 %)		2.272	9.50E-05	HOMO-2 \rightarrow LUMO+3 (17 %)
			HOMO-6 \rightarrow LUMO (14 %)				HOMO-5 \rightarrow LUMO+1 (16 %)
			HOMO-1 \rightarrow LUMO+2 (13 %)				HOMO-6 \rightarrow LUMO (15 %)
γ	2.102	1.17E-03	HOMO-6 \rightarrow LUMO+1 (25 %)		2.284	3.38E-04	HOMO-6 \rightarrow LUMO+1 (12 %)
			HOMO-2 \rightarrow LUMO+5 (22 %)				HOMO-7 \rightarrow LUMO+1 (48 %)
			HOMO-2 \rightarrow LUMO+3 (12 %)				HOMO-2 \rightarrow LUMO+4 (12 %)
	2.106	2.07E-03	HOMO \rightarrow LUMO+5 (10 %)		2.316	9.00E-03	HOMO-6 \rightarrow LUMO+1 (11 %)
			HOMO-6 \rightarrow LUMO+1 (31 %)				HOMO-6 \rightarrow LUMO (11 %)
			HOMO-2 \rightarrow LUMO+5 (21%)				HOMO-1 \rightarrow LUMO+3 (26 %)
	2.131	1.19E-02	HOMO-7 \rightarrow LUMO (11 %)		2.328	1.50E-02	HOMO-5 \rightarrow LUMO (17 %)
			HOMO-2 \rightarrow LUMO+3 (23 %)				HOMO-7 \rightarrow LUMO (43 %)
			HOMO \rightarrow LUMO+5 (17 %)				HOMO-5 \rightarrow LUMO+1 (12 %)
	2.168	9.44E-03	HOMO-6 \rightarrow LUMO+1 (11 %)		2.335	1.42E-02	HOMO-6 \rightarrow LUMO+1 (50 %)
			HOMO-6 \rightarrow LUMO (11 %)				
			HOMO-7 \rightarrow LUMO (54%)				
	2.185	1.58E-02	HOMO-1 \rightarrow LUMO+5 (11 %)				
			HOMO-7 \rightarrow LUMO+1 (62 %)				